The Sixteenth Marcel Grossmann Meeting Downloaded from www.worldscientific.com
by GERMAN ELECTRON SYNCHROTRON @ HAMBURG on 01/30/23. Re-use and distribution is strictly not permitted, except for Open Access articles.

The self-gravitating Fermi gas in Newtonian gravity and general relativity

Pierre-Henri Chavanis

Laboratoire de Physique Théorique, Université de Toulouse, CNRS, UPS, France
E-mail: chavanis@irsamc.ups-tlse.fr

We review the history of the self-gravitating Fermi gas in Newtonian gravity and general relativity. We mention applications to white dwarfs, neutron stars and dark matter halos. We describe the nature of instabilities and phase transitions in the self-gravitating Fermi gas as energy (microcanonical ensemble) or temperature (canonical ensemble) is reduced. When $N < N_{\rm OV}$, where $N_{\rm OV}$ is the Oppenheimer-Volkoff critical particle number, the self-gravitating Fermi gas experiences a gravothermal catastrophe at E_c stopped by quantum mechanics (Pauli's exclusion principle). The equilibrium state has a core-halo structure made of a quantum core (degenerate fermion ball) surrounded by a classical isothermal halo. When $N > N_{\rm OV}$, a new turning point appears at an energy E_c'' below which the system experiences a gravitational collapse towards a black hole [P.H. Chavanis, G. Alberti, Phys. Lett. B **801**, 135155 (2020)]. When $N_{\rm OV} < N < N_*'$, the self-gravitating Fermi gas experiences a gravothermal catastrophe at E_c leading to a fermion ball, then a gravitational collapse at E_c'' leading to a black hole. When $N > N_*'$, the condensed branch disappears and the instability at E_c directly leads to a black hole. We discuss implications of these results for dark matter halos made of massive neutrinos.

Keywords: Fermi-Dirac statistics; White dwarfs; Neutron stars; Dark matter halos; Black holes

1. Introduction

The self-gravitating Fermi gas can have applications in different astrophysical systems ranging from white dwarfs and neutron stars to dark matter halos, where the fermions are electrons, neutrons and massive neutrinos respectively. The study of the self-gravitating Fermi gas is also of fundamental conceptual importance as it combines quantum mechanics and general relativity. Initially, fermionic models were developed at zero temperature ($T = 0$) but they have been later generalized at nonzero temperature, especially in the case of dark matter halos. In these Proceedings, we provide a brief history of the self-gravitating Fermi gas. A more detailed historical account of the statistical mechanics and thermodynamics of self-gravitating systems (classical and quantum) in Newtonian gravity and general relativity can be found in Refs.[1–4].

The statistical equilibrium state of a system of self-gravitating fermions can be determined from a maximum entropy principle. For systems with long-range interactions the mean field approximation becomes exact in an appropriate thermodynamic limit.[3,5] The most probable distribution of an isolated system of self-gravitating fermions at statistical equilibrium is obtained by maximizing the Fermi-Dirac

The Sixteenth Marcel Grossmann Meeting Downloaded from www.worldscientific.com
by GERMAN ELECTRON SYNCHROTRON @ HAMBURG on 01/30/23. Re-use and distribution is strictly not permitted, except for Open Access articles.

entropy S at fixed mass-energy $\mathcal{E} = Mc^2$ and particle number N:

$$\max \left\{ S \quad | \quad \mathcal{E} = Mc^2, \quad N \quad \text{fixed} \right\}. \tag{1}$$

The variational problem for the first variations reads

$$\delta S/k_B - \beta_\infty \delta \mathcal{E} + \alpha \delta N = 0, \tag{2}$$

where $\beta_\infty = 1/k_B T_\infty$ and $\alpha = \mu_\infty / k_B T_\infty$ are Lagrange multipliers associated with the conservation of mass-energy and particle number. Here, T_∞ and μ_∞ represent the temperature and the chemical potential measured by an observer at infinity. The maximization problem (1) is associated with the microcanonical ensemble. If the system is in contact with a thermal bath fixing the temperature T_∞ the statistical equilibrium state is obtained by minimizing the free energy $F = \mathcal{E} - T_\infty S$ at fixed particle number N:

$$\min \left\{ F = \mathcal{E} - T_\infty S \quad | \quad N \quad \text{fixed} \right\}. \tag{3}$$

This minimization problem is associated with the canonical ensemble. At $T = 0$ the equilibrium state is obtained by minimizing the mass-energy $\mathcal{E} = Mc^2$ at fixed particle number N. The equilibrium states in the microcanonical and canonical ensembles are the same. They are determined by the variational principle (2). However, their stability may differ in the two ensembles. This is the notion of ensemble inequivalence for systems with long-range interactions.[3,5] Microcanonical stability implies canonical stability but the converse is wrong.

The equilibrium state of a gas of self-gravitating fermions results from the balance between the repulsion due to the quantum pressure (Pauli's exclusion principle) and the gravitational attraction. The variational principle (2) yields all the equations that we need to determine the equilibrium state of the self-gravitating Fermi gas: (i) the Fermi-Dirac distribution function; (ii) the ideal equation of state of fermions; (iii) the Oppenheimer-Volkoff equations determining the condition of hydrostatic equilibrium in general relativity; (iv) the Tolman-Klein relations expressing how the local temperature $T(r)$ and the local chemical potential $\mu(r)$ are affected by the metric. We can solve these equations numerically and plot the caloric curve $T_\infty(\mathcal{E})$ relating the temperature to the energy. When $T > 0$ we need to enclose the system within a spherical box of radius R in order to prevent its evaporation and have equilibrium states with a finite mass. In the general case, the caloric curve depends on N and R. For convenience, instead of $T_\infty(\mathcal{E})$, we shall plot $\beta_\infty(-E)$ where $E = (M - Nm)c^2$ is the binding energy which reduces to the usual energy $E = K + W$ (kinetic + potential) in the nonrelativistic limit $c \to +\infty$. At $T = 0$, the system is self-confined (without the need of a box) and we shall plot the mass-radius relation $M(R)$ where R denotes here the radius where the density vanishes. The maximum entropy formalism for classical and quantum self-gravitating systems in Newtonian gravity and general relativity is reviewed in Refs.[3,4] where all the equations are derived and an exhaustive list of references is given.

The Sixteenth Marcel Grossmann Meeting Downloaded from www.worldscientific.com
by GERMAN ELECTRON SYNCHROTRON @ HAMBURG on 01/30/23. Re-use and distribution is strictly not permitted, except for Open Access articles.

2. Self-gravitating fermions at $T = 0$

The study of a self-gravitating gas of fermions started in the context of white dwarf stars when Fowler[6] first realized that these compact objects owe their stability to the quantum pressure of the degenerate electron gas. Indeed, the quantum pressure arising from the Pauli exclusion principle is able to counteract the gravitational attraction and explain the very high densities of white dwarf stars. Early studies were devoted to determining the ground state ($T = 0$) of the system. Nonrelativistic white dwarf stars are equivalent to a polytropic gas of index $n = 3/2$. Their density profile can be obtained by solving the Lane-Emden equation numerically. The density profile of white dwarf stars at $T = 0$ has a compact support, i.e., the density vanishes at a finite radius. The mass-radius relation of nonrelativistic white dwarf stars was first obtained by Stoner,[7] Milne[8] and Chandrasekhar.[9a] They showed that the radius of the star decreases as the mass increases according to the law $M = 91.9\,\hbar^6/(G^3 m^8 R^3)$ (see Fig. 1-a).[11] All the configurations of the series of equilibria are stable.

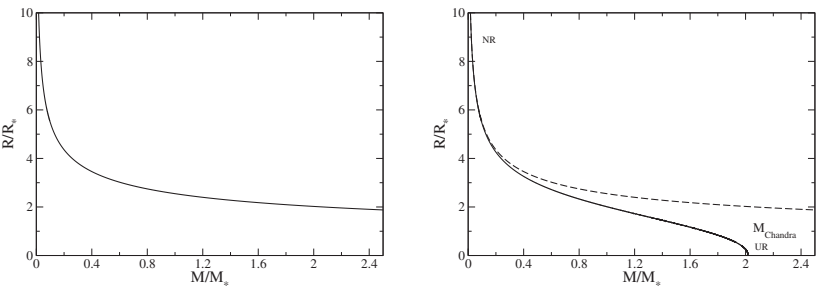

(a) (b)

Fig. 1. Mass-radius relation of self-gravitating fermions at $T = 0$ in Newtonian gravity (the mass is normalized by $M_* = (3\pi/4)^{1/2}\hbar^{3/2}c^{3/2}/(G^{3/2}m^2)$ and the radius by $R_* = (3\pi/4)^{1/2}\hbar^{3/2}/(c^{1/2}G^{1/2}m^2)$). (a) Nonrelativistic white dwarf stars. (b) Special relativistic white dwarf stars.

The fact that relativistic effects become important in white dwarf stars whose mass is of the order of the solar mass was first reported by Frenkel[12] in a not well-known paper. However, he did not consider the implications of this result. Special relativistic effects in white dwarf stars were studied in detail by Anderson,[13] Stoner,[14] Chandrasekhar,[15] and Landau.[16] They found that no equilibrium state is possible above a maximum mass, now known as the Chandrasekhar limit.[b] These authors considered the equation of state of a relativistic Fermi gas at $T = 0$ and

[a]Stoner[7] developed an analytical approach based on a uniform density approximation for the star while Milne[8] and Chandrasekhar[9] developed a numerical approach based on the Lane-Emden theory of polytropes.[10]

[b]See the introduction of Ref.[17] for a short history of the discovery of the maximum mass of white dwarf stars.

The Sixteenth Marcel Grossmann Meeting Downloaded from www.worldscientific.com
by GERMAN ELECTRON SYNCHROTRON @ HAMBURG on 01/30/23. Re-use and distribution is strictly not permitted, except for Open Access articles.

used Newtonian gravity appropriate to white dwarf stars.[c] An ultrarelativistic Fermi gas at $T = 0$ is equivalent to a polytrope of index $n = 3$. Its density profile is obtained by solving the corresponding Lane-Emden equation and it has a compact support. For a polytrope $n = 3$, the mass-radius relation degenerates and indicates that different configurations with an arbitrary radius can exist at the same mass $M_{\rm Chandra} = 3.1\, M_P^3/m^2 = 1.5\, M_\odot$, where $M_P = (\hbar c/G)^{1/2}$ is the Planck mass and m is the proton mass. This argument immediately implies the existence of a critical mass.[15] In a more detailed study, Chandrasekhar[22] considered partially relativistic configurations and numerically obtained the complete mass-radius relation of white dwarf stars, valid for arbitrary densities, joining the nonrelativistic limit to the ultrarelativistic one (see Fig. 1-b).[d] As M approaches $M_{\rm Chandra}$ the radius of the star tends to zero while its density tends to infinity, leading to a Dirac peak. This study unambiguously shows the absence of equilibrium state above a maximum mass. Therefore, the quantum pressure arising from the Pauli exclusion principle cannot balance the gravitational attraction anymore when the star becomes sufficiently relativistic (or when its mass is too large). This is a striking effect of relativity combined with quantum mechanics and gravity. However, the result of Chandrasekhar[22] was severely criticized by Eddington[23] who argued that the absence of equilibrium states above a maximum mass leads to a *reductio ad absurdum* of the formula of relativistic degeneracy. Although the arguments of Eddington were entirely unfounded, his enormous prestige led to an early rejection of Chandrasekhar's work by many in the astronomical community. This pushed Chandrasekhar to abandon the subject, and delayed the discovery of the phenomenon of gravitational collapse and the concept of black hole.

In the following years, similar results were found by Oppenheimer and Volkoff[24] in connection to neutron stars. They solved the equations of general relativity with the relativistic equation of state for fermions at $T = 0$ and found that the mass-radius relation of neutron stars presents a turning point of mass (see Fig. 2).[e] As a result, no equilibrium state exists above a maximum mass $M_{\rm OV} = 0.384\, M_P^3/m^2 = 0.710\, M_\odot$, where m is the neutron mass, called the Oppenheimer-Volkoff limit (note that the density profile with the maximum mass $M_{\rm OV}$ is *not* singular contrary to the Newtonian density profile at the maximum mass $M_{\rm Chandra}$). They argued that, above that mass, the star undergoes gravitational collapse. This problem was specifically studied by Oppenheimer and Snyder[25] who obtained an analytical solution of the Einstein equations describing the collapse of a pressureless gas up to its

[c] In principle, general relativistic effects become important close to the Chandrasekhar maximum mass[18,19] but other phenomena like Coulomb corrections to the electron pressure and the formation of neutrons by inverse beta decay destabilize the star before general relativistic effects come into play.[20,21]

[d] A similar mass-radius relation was obtained earlier by Stoner[14] from an approximate analytical model based on uniform density stars.

[e] It was shown later that the mass-radius relation of neutron stars forms a spiral and that a mode of stability is lost at each turning point of mass.[21]

The Sixteenth Marcel Grossmann Meeting Downloaded from www.worldscientific.com
by GERMAN ELECTRON SYNCHROTRON @ HAMBURG on 01/30/23. Re-use and distribution is strictly not permitted, except for Open Access articles.

Schwarzschild radius. Strangely enough, these important results did not receive much attention until the 1960's. At that epoch, detailed models of compact objects with more realistic equations of state taking into account the repulsive effect of nuclear forces and connecting white dwarfs to neutron stars were constructed and the fundamental discoveries of Chandrasekhar, Landau and Oppenheimer and Volkoff were confirmed (unfortunately, the early contributions of Anderson and Stoner were forgotten).[21] Pulsars were discovered by Hewish *et al.*[26] in 1968. The same year, Gold[27,28] proposed that pulsars are rotating neutron stars, and this is generally accepted today. It is also at that moment that the name "black hole" was used by Wheeler[29] to designate the object resulting from gravitational collapse, and became popular.

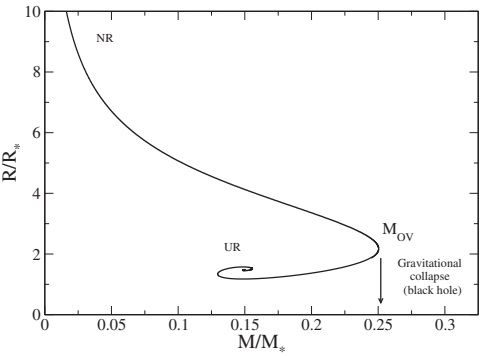

Fig. 2. Mass-radius relation of self-gravitating fermions at $T = 0$ in general relativity (neutron stars).

3. Nonrelativistic classical particles at $T > 0$ and self-gravitating radiation

The thermodynamics of self-gravitating systems is a fascinating subject.[30–32] Its study started with the pioneering work of Antonov[33] who considered an isolated system of nonrelativistic classical particles in gravitational interaction. He used a microcanonical ensemble description in which the mass and the energy are conserved. This situation applies approximately to stellar systems like globular clusters. Their equilibrium state (most probable state) can be obtained by maximizing the Boltzmann entropy S at fixed mass M and energy E.[34] This leads to the mean field Boltzmann distribution which is self-consistently coupled to the Poisson equation. The Boltzmann-Poisson equation was previously introduced and studied in the context of isothermal stars.[10,11] It can be reduced to the Emden equation that has to be solved numerically. Antonov[33] observed that no maximum entropy state exists in an infinite domain (the solution of the Emden equation has an infinite mass), so he proposed to confine the particles within a spherical box of radius R.

The Sixteenth Marcel Grossmann Meeting Downloaded from www.worldscientific.com
by GERMAN ELECTRON SYNCHROTRON @ HAMBURG on 01/30/23. Re-use and distribution is strictly not permitted, except for Open Access articles.

This artifice prevents the evaporation of the system and leads to a well-defined mathematical problem. By computing the second variations of entropy, Antonov[33] showed that equilibrium states with a density contrast $\mathcal{R} = \rho_0/\rho(R) < 709$, where ρ_0 is the central density and $\rho(R)$ the density on the edge of the box, are thermodynamically stable (entropy maxima) while equilibrium states with a density contrast $\mathcal{R} > 709$ are thermodynamically unstable (saddle points of entropy). Lynden-Bell and Wood[35] rediscussed the results of Antonov[33] in more physical terms. They plotted the series of equilibria $E(\mathcal{R})$ and showed that it displays damped oscillations. As a result, there is no equilibrium state with an energy $E < E_c = -0.335\,GM^2/R$, where E_c corresponds to the first turning point of energy (with a density contrast $\mathcal{R}_c = 709$). Invoking the Poincaré turning point criterion,[36] they concluded that the series of equilibria becomes unstable at the minimum energy E_c. In this manner, they recovered the critical density contrast $\mathcal{R}_c = 709$ found by Antonov.[33] They also interpreted the Antonov instability in terms of a "gravothermal catastrophe" caused by the negative specific heat of the system in its densest parts. When this instability occurs, the system undergoes core collapse. This ultimately leads to a binary star surrounded by a hot halo. Lynden-Bell and Wood[35] considered other statistical ensembles, notably the canonical ensemble in which the temperature and the mass are fixed. In that case, the equilibrium state is obtained by minimizing the Boltzmann free energy $F = E - TS$ at fixed mass M. The series of equilibria $T(\mathcal{R})$ displays damped oscillations. No equilibrium state exists with a temperature $T < T_c = 0.397\,GMm/(k_B R)$, where T_c corresponds to the first turning point of temperature (with a density contrast $\mathcal{R}'_c = 32.1$).[f] Using the Poincaré turning point criterion,[36] they concluded that equilibrium states with a density contrast $\mathcal{R} < 32.1$ are thermodynamically stable (free energy minima) while equilibrium states with a density contrast $\mathcal{R} > 32.1$ are thermodynamically unstable (saddle points of free energy). Below T_c the system undergoes an "isothermal collapse" leading to a Dirac peak containing all the particles. Since the stability limits in the microcanonical and canonical ensembles differ, Lynden-Bell and Wood[35] encountered for the first time in statistical mechanics a situation of ensemble inequivalence. This is a peculiarity of systems with long-range interactions.[5] In the present context, it is related to the fact that negative specific heats are allowed in the microcanonical ensemble while they are forbidden in the canonical ensemble.[35] Similar results were obtained independently by Thirring.[37] Katz[38] plotted the caloric curve $\beta(E)$ of isothermal self-gravitating spheres and exhibited its spiral behavior (see Fig. 3-a).[g] He also extended the Poincaré theory on linear series of equilibria[36] to the case where there are several turning points and developed a general method to determine the thermodynamical stability of the equilibrium states from the topology of the caloric

[f] These results were first found by Emden.[10]

[g] This spiral behavior was previously observed for self-gravitating isothermal stars in other representations.[11,39–44] In the present case, it is associated with the damped oscillations of energy and temperature as a function of the density contrast.

The Sixteenth Marcel Grossmann Meeting Downloaded from www.worldscientific.com
by GERMAN ELECTRON SYNCHROTRON @ HAMBURG on 01/30/23. Re-use and distribution is strictly not permitted, except for Open Access articles.

curve $\beta(E)$. A change of stability can only occur at a turning point of energy in the microcanonical ensemble or at a turning point of temperature in the canonical ensemble. A mode of stability is lost if the curve $\beta(-E)$ turns clockwise and gained if it turns anticlockwise. In this manner, one can determine the thermodynamical stability of the system by simply plotting the caloric curve (series of equilibria). The seminal works of Antonov,[33] Lynden-Bell and Wood,[35] and Katz[38] were followed by many other studies (see, e.g., Refs.[45–52]).

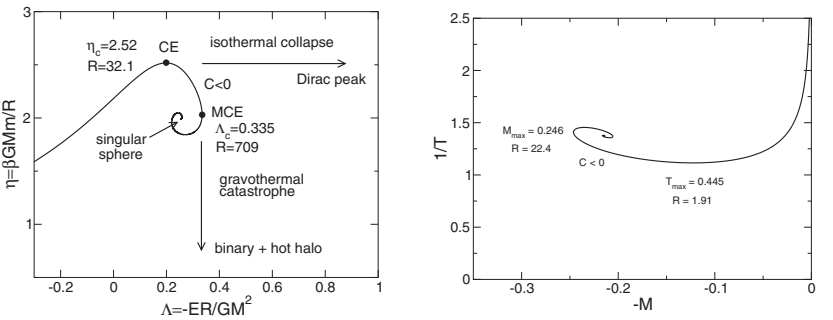

(a) (b)

Fig. 3. (a) Caloric curve of nonrelativistic classical self-gravitating particles (cold spiral).[32] We have plotted the normalized inverse temperature $\eta = \beta GMm/R$ as a function of minus the normalized binding energy $\Lambda = -ER/GM^2$. (b) Caloric curve of the self-gravitating radiation in general relativity (hot spiral).[54] We have plotted the normalized inverse temperature $\hbar^{3/4}c^{7/4}/(k_B T_\infty G^{1/4}R^{1/2})$ as a function of minus the normalized energy $-GM/Rc^2$.

The statistical mechanics of the self-gravitating black-body radiation (photon star) confined within a cavity in general relativity was investigated by Sorkin *et al.*[53] and, more recently, by Chavanis.[54] They showed that the caloric curve $\beta_\infty(\mathcal{E})$ forms a spiral (see Fig. 3-b). There is no equilibrium state above a maximum mass-energy $M_{\max}c^2 = 0.246\, Rc^4/G$ (corresponding to a density contrast 22.4) or above a maximum temperature $(T_\infty)_{\max} = 0.445\, \hbar^{3/4}c^{7/4}/(k_B G^{1/4}R^{1/2})$ (corresponding to a density contrast 1.91). In that case, the system is expected to collapse towards a black hole. We note that the "hot spiral" (see Fig. 3-b) of the self-gravitating radiation in general relativity (ultrarelativistic limit) is inverted with respect to the "cold spiral" of the nonrelativistic classical self-gravitating gas (see Fig. 3-a).

4. Classical particles at $T > 0$ in general relativity

The statistical mechanis of classical particles in general relativity has been considered by Roupas[55] and, independently, by Alberti and Chavanis.[1] The caloric curve depends on one parameter, the particle number N (more precisely N/R). Generically, the caloric curve $\beta_\infty(E)$ has the form of a double spiral (see Fig. 4) which combines the aspects of the "cold spiral" corresponding to a nonrelativistic gas and the aspects of the "hot spiral" corresponding to an ultrarelativistic gas discussed

The Sixteenth Marcel Grossmann Meeting Downloaded from www.worldscientific.com
by GERMAN ELECTRON SYNCHROTRON @ HAMBURG on 01/30/23. Re-use and distribution is strictly not permitted, except for Open Access articles.

in Sec. 3.[h] There is no equilibrium state below a minimum energy (resp. minimum temperature) and above a maximum energy (resp. maximum temperature) in the microcanonical (resp. canonical) ensemble. When the number of particles N increases, the two spirals approach each other, merge, form a loop, and finally disappear (by reducing to a point) at $N_{\max} = 0.1764\, Rc^2/Gm$. For $N > N_{\max}$, there is no equilibrium state whatever the value of mass-energy and temperature.

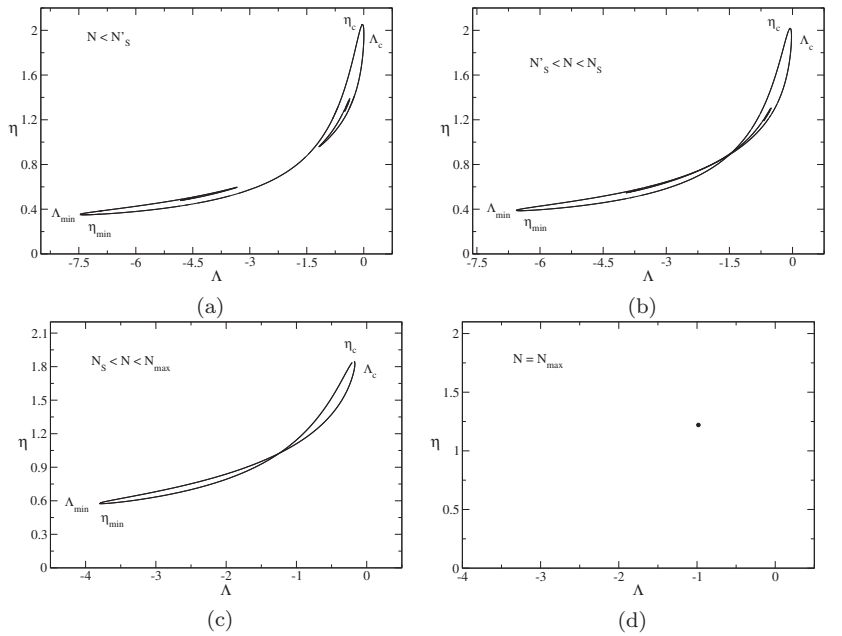

Fig. 4. Caloric curve of classical particles in general relativity. We have plotted the normalized inverse temperature $\eta = \beta_\infty GNm^2/R$ as a function of minus the normalized binding energy $\Lambda = -ER/GN^2m^2$ for different values of the normalized particle number $\nu = GNm/Rc^2$. (a) Double spiral (b) Merging (c) Loop (d) Point.[1]

5. Nonrelativistic fermions at $T > 0$

The statistical mechanics of self-gravitating fermions at nonzero temperature was first studied by Hertel and Thirring[56,57] as a simple (nonrelativistic) model of neutron stars. In that case, the density profile decreases with the distance as r^{-2} and we need to confine the system within a box in order to have an equilibrium state with a finite mass. Hertel and Thirring[56] rigorously proved that the mean field approximation (which amounts to neglecting correlations among the particles) and the Thomas-Fermi approximation (which amounts to neglecting the quantum potential)

[h]The hot spiral of ultrarelativistic classical particles in general relativity is similar, but not identical, to the hot spiral of the self-gravitating radiation.[1,3,54]

The Sixteenth Marcel Grossmann Meeting Downloaded from www.worldscientific.com
by GERMAN ELECTRON SYNCHROTRON @ HAMBURG on 01/30/23. Re-use and distribution is strictly not permitted, except for Open Access articles.

become exact in a proper thermodynamic limit where $N \to +\infty$. This leads to the Fermi-Dirac-Poisson equations, also known as the temperature-dependent Thomas-Fermi equations. Hertel and Thirring[57] solved these equations numerically and plotted the caloric curve. The caloric curve depends on one parameter, the box radius R (more precisely NR^3). They found that, for sufficiently large systems ($R > R_{\rm CCP} = 12.8\,\hbar^2/(N^{1/3}Gm^3)$), a negative specific heat region occurs in the microcanonical ensemble (see Fig. 5). Since negative specific heats are forbidden in the canonical ensemble, this implies that the statistical ensembles are inequivalent. The region of negative specific heats which is allowed in the microcanonical ensemble is replaced by a first order phase transition in the canonical ensemble. This phase transition is expected to take place at a transition temperature T_t connecting the gaseous phase to the condensed phase through a horizontal Maxwell plateau in the caloric curve $T(E)$. This is accompanied by a discontinuity of energy. There is also a lower critical temperature T_c (spinodal point) at which the metastable gaseous phase disappears and the system collapses (zeroth order phase transition). This collapse is associated with the isothermal collapse of classical self-gravitating systems.[10,49] However, for self-gravitating fermions, the collapse stops when quantum degeneracy comes into play. In that case, the system achieves a "core-halo" configuration made of a quantum core (fermion ball) containing almost all the mass surrounded by a tenuous isothermal atmosphere. There is also a higher critical temperature T_* (spinodal point) at which the metastable condensed phase disappears and the system explodes. These results were exported by Bilic and Viollier[58] to the context of dark matter.

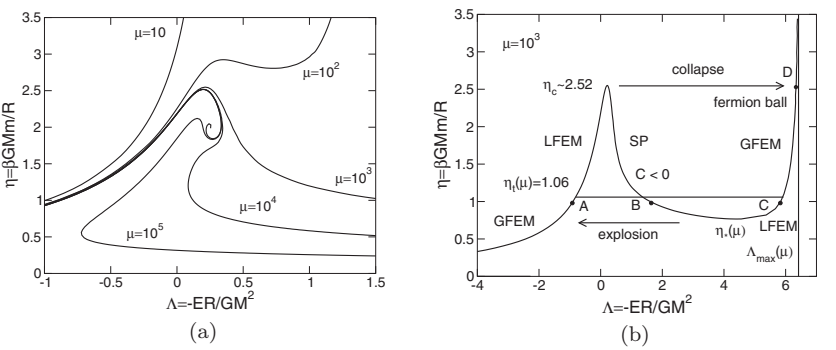

Fig. 5. Caloric curve of nonrelativistic self-gravitating fermions.[32] We have plotted the normalized inverse temperature $\eta = \beta GMm/R$ as a function of minus the normalized energy $\Lambda = -ER/GM^2$ for different values of the normalized radius, or degeneracy parameter $\mu = \eta_0\sqrt{512\pi^4 G^3 MR^3}$, where $\eta_0 = 2m^4/h^3$ is the maximum possible value of the distribution function fixed by the Pauli exclusion principle. (a) Dependence of the series of equilibria on the size of the system. (b) For small systems, the caloric curve has an N-shape structure.

An exhaustive study of phase transitions in the self-gravitating Fermi gas was made by Chavanis[32,59] in both canonical and microcanonical ensembles.

The Sixteenth Marcel Grossmann Meeting Downloaded from www.worldscientific.com
by GERMAN ELECTRON SYNCHROTRON @ HAMBURG on 01/30/23. Re-use and distribution is strictly not permitted, except for Open Access articles.

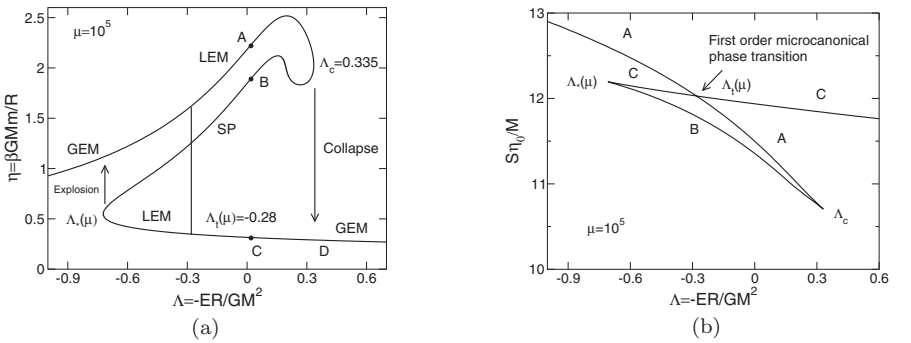

Fig. 6. Caloric curve of nonrelativistic self-gravitating fermions.[32] (a) For large systems, the caloric curve has a Z-shape structure resembling a dinosaur's neck. (b) Illustration of the microcanonical first order phase transition on the $S(E)$ curve.

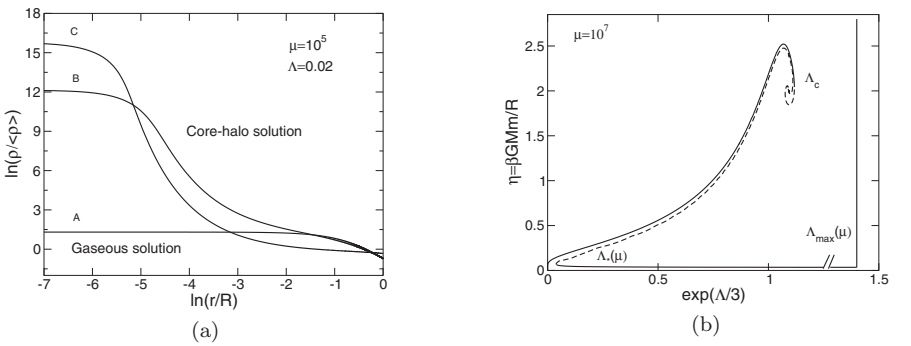

Fig. 7. (a) Density profiles corresponding to the gaseous and core-halo solutions.[32] (b) The classical limit $\mu \to +\infty$ (very large systems).[32] According to the Poincaré-Katz criterion,[36,38] the equilibrium states are unstable in the microcanonical (resp. canonical) ensemble between the first and the last turning points of energy (resp. temperature).

He confirmed the phase transition in the canonical ensemble previously found by Hertel and Thirring[57] and evidenced, for sufficiently large systems ($R > R_{\rm MCP} = 130\,\hbar^2/(N^{1/3}Gm^3)$), a first order phase transition in the microcanonical ensemble (see Fig. 6). This phase transition is expected to take place at a transition energy E_t connecting the gaseous phase to the condensed phase through a vertical Maxwell plateau in the caloric curve $T(E)$. This is accompanied by a discontinuity of temperature. There is also a lower critical energy E_c (spinodal point) at which the metastable gaseous phase disappears and the system collapses (zeroth order phase transition). This collapse is associated with the gravothermal catastrophe of classical self-gravitating systems.[33,35] However, for self-gravitating fermions, the collapse stops when quantum degeneracy comes into play. In that case, the system achieves a core-halo configuration[60] made of a quantum core (fermion ball) containing a moderate fraction of the total mass surrounded by a massive isothermal atmosphere

The Sixteenth Marcel Grossmann Meeting Downloaded from www.worldscientific.com
by GERMAN ELECTRON SYNCHROTRON @ HAMBURG on 01/30/23. Re-use and distribution is strictly not permitted, except for Open Access articles.

(see Fig. 7-a). There is also a higher critical energy E_* (spinodal point) at which the metastable condensed phase disappears and the system explodes. As a result, there exist two distinct critical points in the self-gravitating Fermi gas, one in each ensemble, above which phase transitions occur. For small systems ($R < R_{\rm CCP}$), there is no phase transition, for intermediate size systems ($R_{\rm CCP} < R < R_{\rm MCP}$) a phase transition takes place in the canonical ensemble but not in the microcanoncal ensemble, and for large systems ($R > R_{\rm MCP}$) a phase transition takes place in both ensembles. When $R \to +\infty$, the series of equilibria rotates several times before unwinding (see Fig. 7-b) and we recover the classical spiral from Fig. 3-a. Chavanis[32] determined the phase diagram of the nonrelativistic self-gravitating Fermi gas. He also argued that the lifetime of metastable states is extremely long, scaling as e^N where N is the number of particles, so that the first order phase transitions do not take place in practice.[61] Only zeroth order phase transitions associated with the spinodal points are physically meaningful.

6. General relativistic fermions at $T > 0$

The statistical mechanics of self-gravitating fermions at nonzero temperature in general relativity was first considered by Bilic and Viollier.[62] As before, the system has to be confined within a spherical box of radius R in order to prevent its evaporation. The caloric curve depends on two parameters, the box radius R and the particle number N. Bilic and Viollier[62] studied the case where R is relatively small and $N < N_{\rm OV}$. In that case, the results are qualitatively similar to those obtained for nonrelativistic fermions (see Sec. 5). There is a first order phase transition in the canonical ensemble which replaces the region of negative specific heat present in the microcanonical ensemble. An equilibrium state, which is either "gaseous" (corresponding to the classical isothermal sphere) or "condensed" (made of a fermion ball surrounded by a classical isothermal envelope), exists for any value of temperature T_∞ and binding energy E. General relativistic effects only introduce a small correction to the Newtonian results.

A more general study was performed by Alberti, Chavanis and Roupas[2,63,64] who considered arbitrary values of R and N. When $N > N_{\rm OV}$, they identified the existence of a new turning point of temperature in the canonical ensemble and a new turning point of binding energy in the microcanonical ensemble below which the system collapses and forms a black hole of mass $M_{\rm OV}$ (see Fig. 8). This is the finite temperature generalization of the result originally found by Oppenheimer and Volkoff[24] at $T = 0$. These results lead to the following scenario (we restrict ourselves to the microcanonical ensemble which is the most relevant). At high energies, the system is in the gaseous phase. Below a critical energy E_c it becomes thermodynamically unstable and experiences a gravothermal catastrophe. However, core collapse stops when quantum mechanics (Pauli's exclusion principle) comes into play. This leads to the formation of a fermion ball surrounded by a hot halo. Below E_c'', the condensed phase becomes thermodynamically and dynamically unstable

The Sixteenth Marcel Grossmann Meeting Downloaded from www.worldscientific.com
by GERMAN ELECTRON SYNCHROTRON @ HAMBURG on 01/30/23. Re-use and distribution is strictly not permitted, except for Open Access articles.

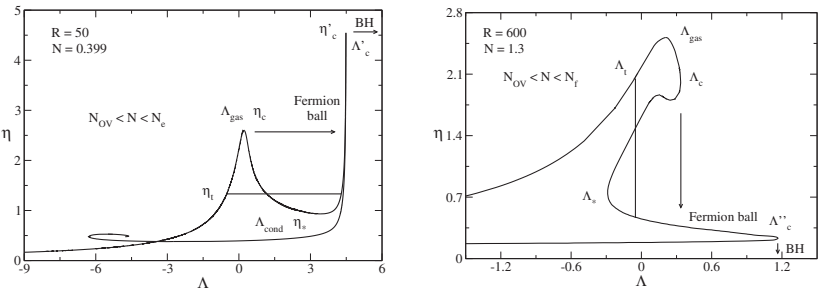

Fig. 8. Caloric curve of self-gravitating fermions in general relativity when $N > N_{\rm OV}$.[2] We have plotted the normalized inverse temperature $\eta = \beta_\infty GNm^2/R$ as a function of minus the normalized binding energy $\Lambda = -ER/GN^2m^2$ for different values of the normalized radius $R/R_{\rm OV}$ and normalized particle number $N/N_{\rm OV}$. (a) Small systems: As T decreases the system experiences an isothermal collapse at T_c leading to a fermion ball, then a gravitational collapse at T_c' leading to a black hole. (b) Large systems: As E decreases the system experiences a gravothermal catastrophe at E_c leading to a fermion ball surrounded by a hot halo, then a gravitational collapse at E_c'' leading to a black hole.

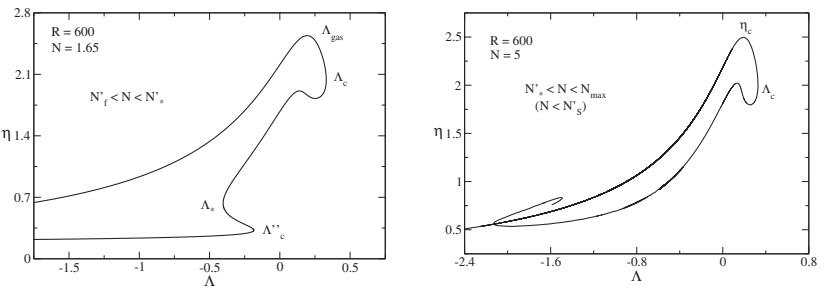

Fig. 9. Caloric curve of self-gravitating fermions in general relativity.[2] When $N > N_*'$ the condensed branch disappears completely so that only the collapse at E_c towards a black hole is possible.

(in a general relativistic sense) and collapses towards a black hole. Alberti and Chavanis[2] also evidenced a critical particle number N_*' above which the condensed phase completely disappears (see Fig. 9). In that case, there is no possibility to form a fermion ball. The gravothermal catastrophe at E_c directly leads to a black hole. In conclusion, for $N < N_{\rm OV}$ the system forms a fermion ball; for $N_{\rm OV} < N < N_*'$ the system generically forms a fermion ball, then (possibly) a black hole; for $N > N_*'$ the system directly forms a black hole. Alberti and Chavanis[2] emphasized the core-halo structure of the equilibrium states in the microcanonical ensemble and mentioned the relation to red-giants (leading to white dwarfs) and supernovae (leading to neutron stars and black holes) suggested in Refs.[64–67]. They also provided the complete phase diagram of the general relativistic Fermi gas.

The Sixteenth Marcel Grossmann Meeting Downloaded from www.worldscientific.com
by GERMAN ELECTRON SYNCHROTRON @ HAMBURG on 01/30/23. Re-use and distribution is strictly not permitted, except for Open Access articles.

7. Truncated models

The study of phase transitions in the self-gravitating Fermi gas can be extended to the fermionic King model described by the distribution function

$$f = A\frac{e^{-\beta(\epsilon-\epsilon_m)}-1}{1+\frac{A}{\eta_0}e^{-\beta(\epsilon-\epsilon_m)}} \qquad (\epsilon \leq \epsilon_m). \tag{4}$$

The fermionic King model was introduced heuristically by Ruffini and Stella[68] as a generalization of the classical King model[69]

$$f = A\left[e^{-\beta(\epsilon-\epsilon_m)}-1\right] \qquad (\epsilon \leq \epsilon_m). \tag{5}$$

The fermionic King model was also introduced independently by Chavanis[70] who derived it from a kinetic theory based on the fermionic Landau equation. The fermionic King model is more realistic than the usual fermionic model because it avoids the need of an artificial box to confine the system. The nonrelativistic fermionic King model was studied by Chavanis *et al.*[71,72] who showed that the density profiles generically have a core-halo structure with a quantum core (fermion ball) and a tidally truncated isothermal halo leading to flat rotation curves.[i] They also studied the caloric curves, the thermodynamical stability of the equilibrium states, and the phase transitions between gaseous and condensed states (see Figs. 10 and 11). They showed that the phenomenology of phase transitions in the fermionic King model is the same as in the case of box-confined systems obtained in Refs.[32,59]. The results of Chavanis *et al.*[72] have been generalized by Argüelles *et al.*[73] to the fermionic King model in general relativity. They also found that the phenomenology of phase transitions in the general relativistic fermionic King model is the same as in the case of box-confined systems obtained in Refs.[2,63,64].

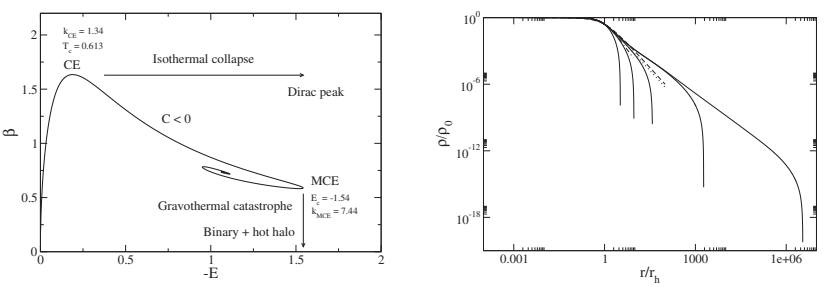

(a) (b)

Fig. 10. (a) Caloric curve of the nonrelativistic classical King model.[71] (b) Density profiles along the series of equilibria.[71] The marginal (critical) King profile at the point of gravothermal instability is relatively close to the Burkert[74] profile (dashed line) which provides a good fit of the density profile of dark matter halos.

[i]The name "fermionic King model" was introduced in Ref.[72].

The Sixteenth Marcel Grossmann Meeting Downloaded from www.worldscientific.com
by GERMAN ELECTRON SYNCHROTRON @ HAMBURG on 01/30/23. Re-use and distribution is strictly not permitted, except for Open Access articles.

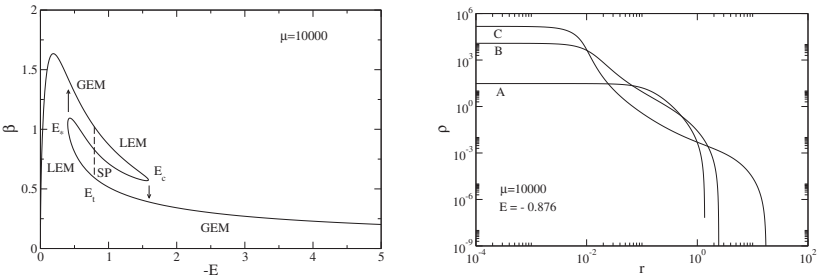

Fig. 11. (a) Caloric curve of the nonrelativistic fermionic King model for large systems.[72] (b) Density profiles corresponding to the stable gaseous phase (A), the stable condensed phase (C), and the unstable intermediate solution (B).[72]

8. Application to dark matter halos

In addition to white dwarfs and neutron stars,[75] the self-gravitating Fermi gas model has been applied in the context of dark matter halos made of massive neutrinos. The suggestion that dark matter is made of massive neutrinos was originally proposed by Markov[76] and Cowsik and McClelland.[77,78] This suggestion has been developed by numerous authors (see the introduction of Ref.[3] for an exhaustive list of references). The first models decribed dark matter halos at $T = 0$ using the equation of state of a completely degenerate fermion gas either in the nonrelativistic limit or in general relativity. Subsequent models considered dark matter halos at nonzero temperature showing that they have a core-halo structure consisting of a dense core (fermion ball) solving the core-cusp problem of classical cold dark matter surrounded by a dilute isothermal atmosphere leading to flat rotation curves. Most models were based on the ordinary Fermi-Dirac distribution in Newtonian gravity or general relativity. Some models were based on the more realistic fermionic King model (describing tidally truncated fermionic dark matter halos). The self-gravitating Fermi gas was also studied in relation to the violent relaxation of collisionless self-gravitating systems described by the Lynden-Bell[79] distribution which is formally similar to the Fermi-Dirac distribution. As argued in Refs.[71,72], the theory of violent relaxation may justify how a collisionless gas of self-gravitating fermions, such as a dark matter halo, can reach a statistical equilibrium state described by the Fermi-Dirac distribution on a timescale smaller than the age of the universe.[j]

The detailed study of the motion of S-stars near the Galactic center has revealed the presence of a very massive central object, Sagittarius A* (Sgr A*). This central object is usually associated with a supermassive black hole (SMBH) of mass

[j]The relaxation time due to close gravitational encounters exceeds the age of the universe by many orders of magnitude. The collisional relaxation time may be shorter if the fermions are self-interacting.[80]

The Sixteenth Marcel Grossmann Meeting Downloaded from www.worldscientific.com by GERMAN ELECTRON SYNCHROTRON @ HAMBURG on 01/30/23. Re-use and distribution is strictly not permitted, except for Open Access articles.

$M = 4.2 \times 10^6\, M_\odot$ and Schwarzschild radius $R_S = 4.02 \times 10^{-7}\,\mathrm{pc}$. Whatever the object may be, its radius must be smaller than $R_\mathrm{P} = 6 \times 10^{-4}\,\mathrm{pc}$ ($R_\mathrm{P} = 1492\, R_S$), the S2 star pericenter. Similar objects are expected to reside at the center of most spiral and elliptical galaxies, in active galactic nuclei (AGN). Although it is commonly believed that these objects are SMBHs, this is not yet established on a firm observational basis in all cases. Some authors have proposed that such objects could be fermion balls or boson stars that could mimic a SMBH. Let us consider this possibility in the framework of the fermionic dark matter model. More precisely, let us investigate if a fermion ball can mimic a SMBH at the center of the Galaxy.

Bilic *et al.*[81] developed a general relativistic model of fermionic dark matter halos at nonzero temperature with a fermion mass $m = 15\,\mathrm{keV/c^2}$ that describes both the center and the halo of the Milky Way in a unified manner. The density profile has a core-halo structure made of a quantum core (fermion ball) surrounded by a classical isothermal atmosphere. The core and the halo are separated by an extended plateau. By using the usual Fermi-Dirac distribution and choosing parameters so as to fit observational data at large distances, they found a fermion ball of mass $M_c = 2.27 \times 10^6\, M_\odot$ and radius $R_c = 18\,\mathrm{mpc}$ and argued that this fermion ball can mimic a SMBH like Sgr A*. Unfortunately, its radius is larger by a factor 100 than the bound $R_P = 6 \times 10^{-4}\,\mathrm{pc}$ set by later observations. This is why Bilic and coworkers abandoned this fermion ball scenario (R. Viollier, private communication). The same problem was encountered later by Ruffini *et al.*[82] who developed a similar model with a fermion mass $m \sim 10\,\mathrm{keV/c^2}$.

More recently, Argüelles *et al.*[83] considered the general relativistic fermionic King model accounting for a tidal confinement. They applied this model to the Milky Way and determined the parameters by fitting the core-halo profile to the observations. For a fermion mass $m = 48\,\mathrm{keV/c^2}$ they obtained a fermion ball of mass $M_c = 4.2 \times 10^6\, M_\odot$ and radius $R_c = R_P = 6 \times 10^{-4}\,\mathrm{pc}$ which, this time, is consistent with the observational constraints of Sgr A*. Therefore, in order to obtain accurate results, it is important to use the fermionic King model[72,83] instead of the usual fermionic model.[32,81,82] Argüelles *et al.*[83] managed to fit the entire density profile and the entire rotation curve of the Milky Way with the fermionic King distribution and argued that a fermion ball can mimic the effect of a SMBH like Sgr A*. This scenario is very attractive because it can explain the whole structure of the galaxy, the supermassive central object and the isothermal halo, by a single distribution (the fermionic King model[68,70]).

Developing the theory of phase transitions in the self-gravitating Fermi gas, Chavanis *et al.*[72] argued that the core-halo solution considered by Bilic *et al.*,[81] Ruffini *et al.*,[82] and Argüelles *et al.*[83] with a small fermion ball mimicking a SMBH surrounded by a classical isothermal atmosphere, which was claimed to reproduce the structure of the Milky Way, is thermodynamically unstable because it lies in the intermediate branch of the caloric curve between the first and the last turning points of energy (see Fig. 7-b). As a result, it is a saddle point of entropy, not an entropy maximum. Therefore, Chavanis *et al.*[72] concluded that this type of solution

The Sixteenth Marcel Grossmann Meeting Downloaded from www.worldscientific.com
by GERMAN ELECTRON SYNCHROTRON @ HAMBURG on 01/30/23. Re-use and distribution is strictly not permitted, except for Open Access articles.

is not likely to result from a natural evolution and, consequently, they questioned the possibility that a fermion ball could mimic a central SMBH.

Following this study,[72] Argüelles *et al.*[73] computed the caloric curve of the fermionic King model in general relativity (see Fig. 12). They showed that the core-halo solution of Ref.[83] which provides a good agreement with the structure of the Milky Way lies just *after* the turning point (b) of energy (see the inset of Fig. 12), so that it is thermodynamically stable in the microcanonical ensemble which is the correct ensemble to consider.[k] This is a very interesting result because it shows that this core-halo structure *may* arise from a natural evolution in the sense of Lynden-Bell. This gives further support to the scenario according to which a fermion ball could mimic a SMBH at the center of the galaxies.

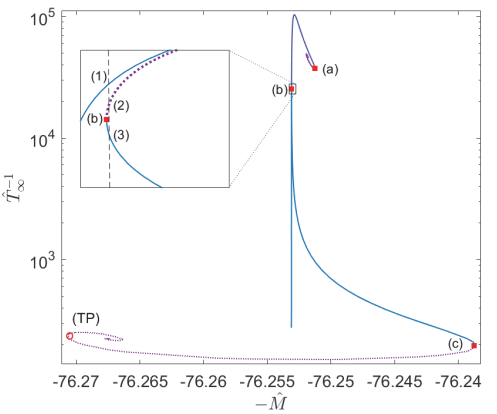

Fig. 12. Caloric curve of the general relativistic fermionic King model (from Ref.[73]).

However, it does not prove that this core-halo structure with a very high central density will necessarily arise from a natural evolution. The reason is that violent relaxation is in general incomplete.[79] The fluctuations of the gravitational potential that are the engine of the collisionless relaxation can die out before the system has reached statistical equilibrium. Therefore, it is not clear if violent relaxation can produce this type of structures.[l] In order to vindicate this scenario, the next step would be to perform direct numerical simulations of collisionless fermionic matter to

[k]Chavanis *et al.*[72] did not focus on the stable branch of condensed states located after point (b) because they argued that these solutions are not astrophysically relevant. Indeed, by considering particular solutions of the condensed branch, they observed that these solutions have a too extended envelope that is not consistent with the structure of dark matter halos (see solution C in Fig. 11-b and Figs. 38-45 of Ref.[72]). Although this claim is correct for most of the solutions on the condensed branch, it turns out that the solutions located just after point (b) *are* astrophysically relevant and correspond to the core-halo solutions studied by Argüelles *et al.*[83]

[l]It may be easier to form core-halo configurations with a very high central density if the fermions are self-interacting and if the Fermi-Dirac equilibrium state results from a collisional relaxation of nongravitational origin instead of a collisionless relaxation as suggested in Ref.[80].

The Sixteenth Marcel Grossmann Meeting Downloaded from www.worldscientific.com
by GERMAN ELECTRON SYNCHROTRON @ HAMBURG on 01/30/23. Re-use and distribution is strictly not permitted, except for Open Access articles.

see if they spontaneously generate fermion balls with the characteristics of SMBHs. A purely gaseous solution without quantum core, which is also a maximum entropy state, may be easier to reach through a violent relaxation process and is consistent with the observations. However, it does not account for a massive central object at the center of the galaxies. In that case, we either have to introduce a primordial SMBH "by hand" or advocate a scenario of gravitational collapse such as the one described below.[80]

For a fermion mass $m = 48\,\mathrm{keV/c^2}$, the mass $M_h = 10^{11}\,M_\odot$ of the Milky Way is larger than the OV mass $M_{\rm OV} = 2.71 \times 10^8\,M_\odot$, so we have to take into account general relativity in the caloric curve. As first shown by Alberti and Chavanis[2,64] for box-confined fermionic systems, and recovered by Argüelles *et al.*[73] for tidally truncated models, relativistic effects create a new turning point of energy in the caloric curve at which the condensed branch terminates (see Figs. 8, 9 and point (c) in Fig. 12). Below E_c'' the system collapses towards a black hole.

Suppose that violent relaxation selects the gaseous solution. On a secular timescale, because of collisions, the system follows the upper branch of the series of equilibria (gaseous states) up to the point of minimum energy E_c. At that point, it becomes thermodynamically unstable and undergoes a gravothermal catastrophe. However, core collapse is stopped by quantum mechanics, leading to the formation of a fermion ball. Then, if the energy keeps decreasing, the system follows the lower branch of the series of equilibria up to the point of minimum energy E_c'' where it becomes thermodynamically and dynamically unstable (in a general relativistic sense) and collapses towards a SMBH of mass $M_{\rm OV}$. A similar outcome arises if violent relaxation selects the core-halo solution where the fermion ball mimics a SMBH. On a secular timescale, the system follows the lower branch of the series of equilibria up to the point of minimum energy E_c'' at which it collapses towards a SMBH. In the two cases, the ultimate fate of the system is to form a SMBH of mass $M_{\rm OV}$ surrounded by an envelope. However, the formation of a SMBH may take time (more than the age of the universe) so that the two objects (fermion ball or SMBH) are possible in practice.

For a fermion mass $m = 48\,\mathrm{keV/c^2}$, the OV mass $M_{\rm OV} = 2.71 \times 10^8\,M_\odot$ is too large to account for the mass of a SMBH like Sgr A* at the center of the Milky Way. This suggests that the object at the center of the Galaxy (Sgr A*) is a fermion ball instead of a SMBH as argued by Argüelles *et al.*[73] However, for very large halos ($N > N_*'$), it is shown by Alberti and Chavanis[2] that the condensed branch disappears (see panel (b) of Fig. 9). In that case, there is no stable solution with a fermion ball and the system necessarily collapses towards a SMBH. Therefore, medium size galaxies like the Milky Way should harbor a fermion ball of mass $M_c = 4.2 \times 10^6\,M_\odot$ while very large galaxies like ellipticals should harbor a SMBH of mass $M_{\rm OV} = 2.71 \times 10^8\,M_\odot$ that could even grow by accretion. This scenario[80] could account for the mass of SMBHs in AGNs like the one recently photographed in M87 ($M_h \sim 10^{13}\,M_\odot$ and $M_{\rm BH} \sim 10^{10}\,M_\odot$).

The Sixteenth Marcel Grossmann Meeting Downloaded from www.worldscientific.com
by GERMAN ELECTRON SYNCHROTRON @ HAMBURG on 01/30/23. Re-use and distribution is strictly not permitted, except for Open Access articles.

On the other hand, for a much larger fermion mass $m = 386\,\mathrm{keV/c^2}$, the OV mass $M_{\mathrm{OV}} = 4.2 \times 10^6\,M_\odot$ is comparable to the mass of Sgr A*. Furthermore, when applied to the Milky Way, the caloric curve corresponding to $m = 386\,\mathrm{keV/c^2}$ is similar to the one reported in panel (b) of Fig. 9 so there is no possibility to form a fermion ball. In that case, the Milky Way could have undergone a gravitational collapse at E_c leading to a SMBH of mass $M_{\mathrm{OV}} = 4.2 \times 10^6\,M_\odot$.[80] In this process, the halo surrounding the SMBH is left undisturbed and could correspond to a marginal classical King profile, which is known[71,72] to give a good agreement with the empirical Burkert[74] profile of observed dark matter halos (see Fig. 10-b).

Different scenarios are possible depending on the value of the fermion mass m. Argüelles *et al.*[73,83] determined the mass of the fermionic dark matter particle in such a way that the fermion ball that would be at the center of a large fermionic dark matter halo, like the one that surrounds the Milky Way, mimics the effect of a SMBH of mass $M_c = 4.2 \times 10^6\,M_\odot$ and radius $R_c = 6 \times 10^{-4}\,\mathrm{pc}$ like Sgr A*. This leads to a fermion mass $m = 48\,\mathrm{keV/c^2}$.[m] Alternatively, Chavanis[80,86] determined the mass of the fermionic dark matter particle by arguing that the smallest halos observed in the universe (dSphs like Fornax) with a typical mass $M \sim 10^8\,M_\odot$ and a typical radius $R \sim 1\,\mathrm{kpc}$ represent the ground state of the self-gravitating Fermi gas at $T = 0$. This yields a much smaller fermion mass $m = 165\,\mathrm{eV/c^2}$. When this model is applied to the Milky Way,[80] it leads to a large fermion ball of mass $M_c = 9.45 \times 10^9\,M_\odot$ and radius $R_c = 240\,\mathrm{pc}$. Therefore, it predicts the existence of a large dark matter bulge at the center of the Galaxy instead of a compact fermion ball mimicking a SMBH.[n] A large dark matter bulge is not inconsistent with the observations and may even solve some issues. For example, De Martino *et al.*[87] have argued that the presence of a bosonic dark matter bulge (soliton) of mass $M_c \simeq 10^9\,M_\odot$ and radius $R_c \simeq 100\,\mathrm{pc}$ at the center of the Galaxy may account for the dispersion velocity peak observed in the Milky Way. A large dark matter bulge made of fermions should have the same effect.[80]

Finally, we mention potential difficulties or, alternatively, potentially important predictions associated with the model of Argüelles *et al.*[73,83] If the fermion mass is $m = 48\,\mathrm{keV/c^2}$, dark matter halos of mass $M_h = 10^8\,M_\odot$ such as dSphs like Fornax should have a very pronounced core-halo structure since they do not correspond to the ground state of the self-gravitating Fermi gas (unlike the model of Ref.[80] with $m = 165\,\mathrm{eV/c^2}$). More precisely, the fermionic dark matter model with a fermion mass $m = 48\,\mathrm{keV/c^2}$ predicts that dSphs of mass $M_h = 10^8\,M_\odot$ should contain a fermion ball of mass $M_c = 1.57 \times 10^4\,M_\odot$ and radius $R_c = 5.42\,\mathrm{mpc}$ possibly

[m] In very recent works, Becerra-Vergara *et al.*[84,85] showed that the gravitational potential of a fermion ball (with a particle mass $m = 56\,\mathrm{keV/c^2}$) leads to a better fit of the orbits of all the 17 best resolved S-stars orbiting Sgr A* (including the S2 and G3 objects) with respect to the one obtained by the central SMBH model.

[n] In that case, a primordial SMBH has to be introduced "by hand" at the center of the Galaxy in order to account for the presence of Sgr A*.

The Sixteenth Marcel Grossmann Meeting Downloaded from www.worldscientific.com
by GERMAN ELECTRON SYNCHROTRON @ HAMBURG on 01/30/23. Re-use and distribution is strictly not permitted, except for Open Access articles.

mimicking an intermediate mass black hole.[80] This result is consistent with the detailed work of Argüelles *et al.*[88] who obtained dense cores of mass between $M_c = 10^3\,M_\odot$ and $M_c = 10^6\,M_\odot$ depending on the central effective temperature of the fermions. This is either a very important prediction (if confirmed by observations) or the evidence that this model is incorrect (if invalidated by observations). It would be extremely important to clarify this issue by confronting the model of Argüelles *et al.*[73,83] to ultracompact halos in order to determine which of the two models (the model of Argüelles *et al.*[73,83] with $m = 48\,\mathrm{keV/c^2}$ or the one developed by Chavanis[80] with $m = 165\,\mathrm{eV/c^2}$ or $m \sim 1\,\mathrm{keV}/c^2$) is the most relevant for dark matter halos.

9. Conclusion

In these Proceedings, we have provided a brief history of the self-gravitating Fermi gas in Newtonian gravity and general relativity. We have focused exclusively on papers that discuss the caloric curves and the mass-radius relations of the self-gravitating Fermi gas. We have shown how these curves become more and more complex, displaying various types of phase transitions and instabilities, when gravity effects, thermal effects, quantum effects, relativity effects and tidal effects are progressively taken into account. Of course, there are many more interesting papers on self-gravitating fermions that are not reviewed here. A detailed bibliography on the subject can be found in Refs.[3,80] and in standard textbooks of astrophysics.

We have applied the self-gravitating Fermi gas model to dark matter halos. The Fermi-Dirac distribution may be justified either from the theory of collisionless violent relaxation[72,79] or from a collisional relaxation of nongravitational origin if the fermions are self-interacting.[80] If the fermions have a small mass ($m \lesssim 1\,\mathrm{keV}/c^2$), the caloric curve applied to the Milky Way has an N-shape structure (see Fig. 5-b) and the equilibrium states display a large quantum bulge of mass $M_c \sim 10^{10}\,M_\odot$ and radius $R_c \sim 100\,\mathrm{pc}$ surrounded by an isothermal atmosphere similar to the Burkert profile.[80] If the fermions have a large mass ($m \sim 50\,\mathrm{keV}/c^2$), the caloric curve has a Z-shape structure (see Fig. 6-a). It displays a nonrelativistic turning point of energy at E_c triggering the gravothermal catastrophe. For nonrelativistic fermions, the gravothermal catastrophe is stopped by quantum degeneracy (Pauli's exclusion principle).[60] This may lead to a compact fermion ball of mass $M_c \sim 4.2 \times 10^6\,M_\odot$ and radius $R_c \sim 6 \times 10^{-4}\,\mathrm{pc}$ mimicking a SMBH surrounded by an isothermal atmosphere.[73] When $N > N_{\rm OV}$, which is the case for the Milky Way, a new turning point of energy appears at E_c'' due to general relativity (see Figs. 8-b and 12). It triggers a gravitational collapse towards a SMBH. This new turning point of energy was first evidenced in Refs.[2,63,64] for box-confined fermions and confirmed in Ref.[73] for the fermionic King model. The possibility to form either a fermion ball or a SMBH at the center of the galaxies depends on the size of the galaxy. In medium size galaxies like the Milky Way (when $N < N_*'$) we expect to form a fermion ball of mass $M_c \sim 4.2 \times 10^6\,M_\odot$ but in large galaxies (when $N > N_*'$) the condensed branch

The Sixteenth Marcel Grossmann Meeting Downloaded from www.worldscientific.com
by GERMAN ELECTRON SYNCHROTRON @ HAMBURG on 01/30/23. Re-use and distribution is strictly not permitted, except for Open Access articles.

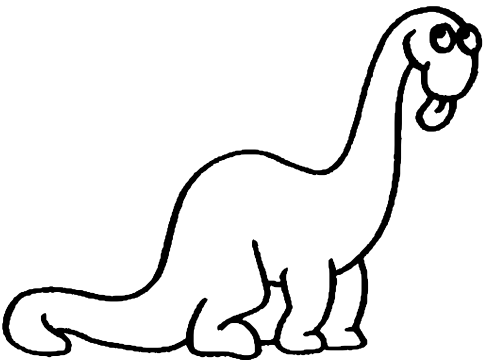

Fig. 13. Dinosaur (artistic view) similar to Fig. 6-a.

disappears (see Fig. 9-b) and the gravothermal catastrophe necessarily results in the formation of a SMBH of mass $M_{\rm OV} \sim 10^8\, M_\odot$.

It is interesting to study the effect of the dimension of space d on phase transitions in the self-gravitating Fermi gas. This is done in Refs.[17,89–91]. In particular, it is shown that fermion stars are unstable in a universe with $d \geq 4$ dimensions. In that case, quantum mechanics cannot stabilize matter against gravitational collapse even in the nonrelativistic regime.[17,89,90] This is similar to a result found by Ehrenfest[92] who considered the effect of the dimension of space on the laws of physics and showed that planetary motion and the Bohr atom would not be stable in a space of dimension $d \geq 4$. Therefore, the dimension $d = 3$ of our Universe is very particular with possible implications regarding the Anthropic Principle.

Finally, it is interesting to compare the results obtained for fermion stars with those obtained for boson stars and self-gravitating Bose-Einstein condensates (BECs) (see our contribution[93] in these Proceedings). Similarly to fermionic dark matter halos, BEC dark matter halos also have a core-halo structure in which the "fermion ball" is replaced by a "soliton". The analogy between fermionic and bosonic dark matter halos is discussed in Refs.[80,86,94].

References

1. G. Alberti, P.H. Chavanis, Phys. Rev. E **101**, 052105 (2020).
2. G. Alberti, P.H. Chavanis, Eur. Phys. J. B **93**, 208 (2020).
3. P.H. Chavanis, Eur. Phys. J. Plus **135**, 290 (2020).
4. P.H. Chavanis, Eur. Phys. J. Plus **135**, 310 (2020).
5. A. Campa, T. Dauxois, D. Fanelli, S. Ruffo, *Physics of Long-Range Interacting Systems* (Oxford University Press, 2014).
6. R.H. Fowler, Mon. Not. R. Astron. Soc. **87**, 114 (1926).
7. E.C. Stoner, Phil. Mag. **7**, 63 (1929).
8. E.A. Milne, Mon. Not. R. Astron. Soc. **91**, 4 (1930).
9. S. Chandrasekhar, Phil. Mag. **11**, 592 (1931).
10. R. Emden, *Gaskugeln* (Leipzig, 1907).

The Sixteenth Marcel Grossmann Meeting Downloaded from www.worldscientific.com
by GERMAN ELECTRON SYNCHROTRON @ HAMBURG on 01/30/23. Re-use and distribution is strictly not permitted, except for Open Access articles.

11. S. Chandrasekhar, *An Introduction to the Theory of Stellar Structure* (University of Chicago Press, 1939).
12. J. Frenkel, Z. Phys. **50**, 234 (1928).
13. W. Anderson, Zeit. f. Phys. **56**, 851 (1929).
14. E.C. Stoner, Phil. Mag. **9**, 944 (1930).
15. S. Chandrasekhar, Astrophys. J. **74**, 81 (1931).
16. L.D. Landau, Phys. Zeit. Sow. **1**, 285 (1932).
17. P.H. Chavanis, Phys. Rev. D **76**, 023004 (2007).
18. S.A. Kaplan, Naukovy Zapiski (Sci. Notes Univ. Lwow) **15**, 109 (1949).
19. S. Chandrasekhar, R.F. Tooper, Astrophys. J. **139**, 1396 (1964).
20. T. Hamada, E.E. Salpeter, Astrophys. J. **134**, 683 (1961).
21. B.K. Harrison, K.S. Thorne, M. Wakano, J.A. Wheeler, *Gravitation Theory and Gravitational Collapse*, (Chicago University Press, Chicago, 1965).
22. S. Chandrasekhar, Mon. Not. R. Astron. Soc. **95**, 207 (1935).
23. A.S. Eddington, Mon. Not. R. Astron. Soc. **95**, 194 (1935).
24. J.R. Oppenheimer, G.M. Volkoff, Phys. Rev. **55**, 374 (1939).
25. J.R. Oppenheimer, H. Snyder, Phys. Rev. **56**, 455 (1939).
26. A. Hewish, S.J. Bell, J.D.H. Pilkington, P.F. Scott, R.A. Collins, Nature **217**, 709 (1968).
27. T. Gold, Nature **218**, 731 (1968).
28. T. Gold, Nature **221**, 25 (1969).
29. J.A. Wheeler, American Scientist **56**, 1 (1968).
30. T. Padmanabhan, Phys. Rep. **188**, 285 (1990).
31. J. Katz, Found. Phys. **33**, 223 (2003).
32. P.H. Chavanis, Int. J. Mod. Phys. B **20**, 3113 (2006).
33. V.A. Antonov, Vest. Leningr. Gos. Univ. **7**, 135 (1962).
34. K.F. Ogorodnikov, *Dynamics of Stellar Systems* (Pergamon, 1965).
35. D. Lynden-Bell, R. Wood, Mon. Not. R. Astron. Soc. **138**, 495 (1968).
36. H. Poincaré, Acta Math. **7**, 259 (1885).
37. W. Thirring, Z. Physik **235**, 339 (1970).
38. J. Katz, Mon. Not. R. Astron. Soc. **183**, 765 (1978).
39. S. Chandrasekhar, Astrophys. J. **87**, 535 (1938).
40. L.R. Henrich, S. Chandrasekhar, Astrophys. J. **94**, 525 (1941).
41. M. Schönberg, S. Chandrasekhar, Astrophys. J. **96**, 161 (1942).
42. R. Ebert, Z. Astrophys. **37**, 217 (1955).
43. W.B. Bonnor, Mon. Not. R. Astron. Soc. **116**, 351 (1956).
44. W.H. McCrea, Mon. Not. R. Astron. Soc. **117**, 562 (1957).
45. T. Padmanabhan, Astrophys. J. Supp. **71**, 651 (1989).
46. H.J. de Vega, N. Sanchez, F. Combes, Phys. Rev. D **54**, 6008 (1996).
47. H.J. de Vega, N. Sanchez, Nucl. Phys. B **625**, 409 (2002).
48. H.J. de Vega, N. Sanchez, Nucl. Phys. B **625**, 460 (2002).
49. P.H. Chavanis, Astron. Astrophys. **381**, 340 (2002).
50. P.H. Chavanis, Astron. Astrophys. **401**, 15 (2003).
51. J. Katz, I. Okamoto, Mon. Not. R. Astron. Soc. **317**, 163 (2000).
52. P.H. Chavanis, Astron. Astrophys. **432**, 117 (2005).
53. R.D. Sorkin, R.M. Wald, Z.Z. Jiu, Gen. Relat. Grav. **13**, 1127 (1981).
54. P.H. Chavanis, Astron. Astrophys. **483**, 673 (2008).
55. Z. Roupas, Class. Quantum Grav. **32**, 135023 (2015).
56. P. Hertel and W. Thirring, Commun. Math. Phys. **24**, 22 (1971).

The Sixteenth Marcel Grossmann Meeting Downloaded from www.worldscientific.com
by GERMAN ELECTRON SYNCHROTRON @ HAMBURG on 01/30/23. Re-use and distribution is strictly not permitted, except for Open Access articles.

57. P. Hertel and W. Thirring, Thermodynamic Instability of a System of Gravitating Fermions. In: H.P. Dürr (Ed.): *Quanten und Felder* (Brauschweig: Vieweg 1971).
58. N. Bilic, R.D. Viollier, Phys. Lett. B **408**, 75 (1997).
59. P.H. Chavanis, Phys. Rev. E **65**, 056123 (2002).
60. P.H. Chavanis, J. Sommeria, Mon. Not. R. Astron. Soc. **296**, 569 (1998).
61. P.H. Chavanis, Astron. Astrophys. **432**, 117 (2005).
62. N. Bilic, R.D. Viollier, Eur. Phys. J. C **11**, 173 (1999).
63. Z. Roupas, P.H. Chavanis, Class. Quant. Grav. **36**, 065001 (2019).
64. P.H. Chavanis, G. Alberti, Phys. Lett. B **801**, 135155 (2020).
65. Y. Pomeau, M. Le Berre, P.H. Chavanis and B. Denet, Eur. Phys. J. E **37**, 26 (2014).
66. P.H. Chavanis, B. Denet, M. Le Berre and Y. Pomeau, Eur. Phys. J. B **92**, 271 (2019).
67. P.H. Chavanis, B. Denet, M. Le Berre and Y. Pomeau, Eur. Phys. Lett. **129**, 30003 (2020).
68. R. Ruffini, L. Stella, Astron. Astrophys. **119**, 35 (1983).
69. I.R. King, Astron. J. **70**, 376 (1965).
70. P.H. Chavanis, Mon. Not. R. Astron. Soc. **300**, 981 (1998).
71. P.H. Chavanis, M. Lemou, F. Méhats, Phys. Rev. D **91**, 063531 (2015).
72. P.H. Chavanis, M. Lemou, F. Méhats, Phys. Rev. D **92**, 123527 (2015).
73. C.R. Argüelles, M.I. Díaz, A. Krut, R. Yunis, Mon. Not. R. astr. Soc. **502**, 4227 (2021).
74. A. Burkert, Astrophys. J. **447**, L25 (1995).
75. S.L. Shapiro, S.A. Teukolsky *Black Holes, White Dwarfs, and Neutron Stars* (Wiley Interscience, 1983).
76. M.A. Markov, Phys. Lett. **10**, 122 (1964).
77. R. Cowsik and J. McClelland, Phys. Rev. Lett. **29**, 669 (1972).
78. R. Cowsik and J. McClelland, Astrophys. J. **180**, 7 (1973).
79. D. Lynden-Bell, Mon. Not. Roy. Astr. Soc. **136**, 101 (1967).
80. P.H. Chavanis, *Predictive model of fermionic dark matter halos with a quantum core and an isothermal atmosphere*, preprint
81. N. Bilic, G.B. Tupper, R.D. Viollier, Lect. Notes Phys. **616**, 24 (2003).
82. R. Ruffini, C.R. Argüelles, J.A. Rueda, Mon. Not. R. Astron. Soc. **451**, 622 (2015).
83. C.R. Argüelles, A. Krut, J.A. Rueda, R. Ruffini, Phys. Dark Univ. **21**, 82 (2018).
84. E.A. Becerra-Vergara, C.R. Argüelles, A. Krut, J.A. Rueda, R. Ruffini, Astron. Astrophys. **641**, A34 (2020).
85. E.A. Becerra-Vergara, C.R. Argüelles, A. Krut, J.A. Rueda, R. Ruffini, Mon. Not. Roy. Astr. Soc. **505**, L64 (2021).
86. P.H. Chavanis, Phys. Rev. D **100**, 123506 (2019).
87. I. De Martino, T. Broadhurst, S.H. Henry Tye, T. Chiueh, H.Y. Schive, Phys. Dark Univ. **28**, 100503 (2020).
88. C.R. Argüelles, A. Krut, J.A. Rueda, R. Ruffini, Phys. Dark Univ. **24**, 100278 (2019).
89. P.H. Chavanis, Phys. Rev. E **69**, 066126 (2004).
90. P.H. Chavanis, C. R. Physique **7**, 331 (2006).
91. M. Kirejczyk, G. Müller, P.H. Chavanis, arXiv:2110.01044
92. P. Ehrenfest, Proc. Amst. Acad. **20**, 200 (1917).
93. P.H. Chavanis, *The maximum mass of dilute axion stars*, preprint.
94. P.H. Chavanis, Phys. Rev. D **100**, 083022 (2019).